Available online at www.sciencedirect.com
ScienceDirect
Trans. Nonferrous Met. Soc. China 26(2016) 2029−2042
Transactions of Nonferrous Metals Society of China
www.tnmsc.cn

Microstructural evolution and mechanical properties of thixoformed A319 alloys containing variable amounts of magnesium

M. S. SALLEH[1], M. Z. OMAR[2], K. S. ALHAWARI[2], M. N. MOHAMMED[3], M. A. MAD ALI[1], E. MOHAMAD[1]

1. Department of Manufacturing Process, Faculty of Manufacturing Engineering, Universiti Teknikal Malaysia Melaka, Hang Tuah Jaya, 76100 Durian Tunggal Melaka, Malaysia;
2. Department of Mechanical and Materials Engineering, Faculty of Engineering and Built Environment, Universiti Kebangsaan Malaysia, 43600, Selangor, Malaysia;
3. Department of Engineering and Technology, Faculty of Information Sciences and Engineering, Management and Science University, 40100 Shah Alam, Selangor, Malaysia

Received 7 September 2015; accepted 7 December 2015

Abstract: The effects of Mg content on the microstructure and tensile properties of thixoformed A319 alloys were studied. The samples were thixoformed at 50% liquid content and some of the thixoformed samples were subjected to the T6 heat treatment. The samples were then examined by optical microscopy (OM), scanning electron microscopy (SEM), energy dispersive X-ray (EDX) spectroscopy and X-ray diffraction (XRD) analysis as well as tensile tests. The results showed that magnesium was able to refine the eutectic silicon in the samples. It was also observed that a compact $Al_9FeMg_3Si_5$ phase was formed when the magnesium content was 1.0% and 1.5%. The results also revealed that as the magnesium content in the alloy increases, the tensile strengths of the thixoformed alloys also increase. The ultimate tensile strength, yield strength and elongation to fracture of the thixoformed A319 heat treated alloy were 298 MPa, 201 MPa and 4.5%, respectively, whereas the values of the thixoformed heat treated alloy with 1.5% Mg content were 325 MPa, 251 MPa and 1.4%, respectively. Thixoformed A319 alloy showed a dimple fracture behaviour, while thixoformed A319 alloys with 1.5% Mg showed a mixed mode fracture behaviour, where dimple and cleavage ruptures were seen on the fracture surface of the samples.

Key words: aluminium alloy; thixoforming; T6 heat treatment; mechanical properties

1 Introduction

A319 aluminium alloy is increasingly being used by the automotive industry to produce engine components. This type of alloy offers a high degree of strength with excellent castability, light weight and good machinability [1,2]. The microstructural constituents present in this alloy are typically complex multiphase comprising eutectic Si and also numerous intermetallic phases such as Al_2Cu, Mg_2Si, $Al_9FeMg_3Si_5$, β-Al_5FeSi and $Al_5Cu_2Mg_8Si_5$ [3,4]. In recent years, the need to produce near net-shape products that have superior properties to those produced by the conventional casting process has drawn attention towards a new processing technique known as semi-solid metal (SSM) processing [5]. This type of processing offers a solution to the problems associated with die casting due to its capability of using a lower temperature than that required by die casting [6,7]. It also uses low forming forces during the shaping process [8]. Moreover, this process also ameliorates the usage of feedstock materials and contributes to the diminution of the cost of processing manufactured parts [9,10].

One type of SSM processing is thixoforming, which involves the preparation of suitable feedstock alloys, re-heating them to a semi-solid state and then forming near net-shaped products [11,12]. This process has an advantage not only in enhancing the tensile strength of the alloy, but also in augmenting the corrosion resistance of the alloy which is essential for automotive industry. It has been reported that corrosion properties of aluminium alloys were improved by thixoforming process compared to rheocast and gravity-cast samples [13]. Among the SSM processing techniques for nondendritic feedstock production, cooling slope (CS) casting is one of the most

Corresponding author: M. S. SALLEH; E-mail: shukor@utem.edu.my
DOI: 10.1016/S1003-6326(16)64321-2

suitable techniques to obtain fine globular primary particles with a high degree of sphericity [14,15]. This technique involves pouring the molten metal over an inclined plate with circulating water underneath so that nucleation occurs during the flow of the liquid, thereby producing a fine and less dendritic microstructure [16]. Cost effectiveness and simplicity are the major advantages of using the CS technique. Additionally, it can be used with ease [17,18]. Various studies have reported on the effects of Mg and ageing on the mechanical properties of A319 aluminium alloys. According to ALKAHTANI [19], increasing the Mg content up to 0.45% in A319 alloy improves the alloy's response to T6 heat treatment, which provides the best combination of mechanical properties. Therefore, increasing the Mg content in A319 alloy can improve the mechanical properties of these alloys, which are suitable for automotive applications.

T6 heat treatment is usually used to enhance the mechanical properties of Al−Si−Cu alloys. The standard T6 heat treatment consists of three stages: solution treatment, water quenching, and artificial ageing. Solution treatment of the alloy is normally performed at more than 500 °C in order to dissolve the solutes atom, which is responsible for the hardening response. Quenching is then used to maintain the desired condition of the supersaturated solid solution at low temperature. Artificial ageing consists of further heating the alloy at low temperature (at approximately 158 °C) and during this stage, the precipitation of dissolved elements occurs. These precipitates are responsible for the hardening of the A319 alloy. The hardening during artificial ageing that occurs by the cooperative precipitation of the Al_2Cu and Mg_2Si phases results in a tremendous improvement in the mechanical properties of the alloy relative to those of non-heat treated alloys [20]. Moreover, the reaction of Mg with Fe results in the formation of the π-$Al_8FeMg_3Si_6$ compound, which is less harmful than the β-Al_5FeSi compound. These compounds reduce the tensile strength and ductility of the materials [21].

Most works on the effect of Mg on the mechanical properties of A319 alloys have focused on conventional cast alloys. In contrast, there has been very limited work on the effect of Mg on alloys formed by thixoforming process. Therefore, the present study was undertaken to investigate the effect of different Mg content (0.3%, 1.0% and 1.5%) on the microstructure and mechanical properties of thixoformed A319 alloys. The alloys were produced using a CS casting method, before they were thixoformed in a compression press. The effects of T6 heat treatment on the mechanical properties and fracture behaviour of the thixoformed alloys were also investigated.

2 Experimental

Al−6.3Si−3.0Cu−xMg (x=0.3, 1.0, 1.5, mass fraction, %) alloys were fabricated by using a conventional casting process to obtain the alloy composition as depicted in Table 1. The experimental flow process for this research is illustrated in Fig. 1.

Table 1 Chemical compositions of studied alloys (mass fraction, %)

Alloy	Si	Cu	Mg	Mn	Zn	Ni	Fe	Cr	Ti	Al
A319	6.26	2.91	0.31	0.15	0.71	0.06	0.53	0.03	0.03	Bal.
TH1	6.31	2.92	0.92	0.11	0.54	0.04	0.45	0.03	0.01	Bal.
TH2	6.15	2.95	1.46	0.10	0.66	0.03	0.48	0.03	0.05	Bal.

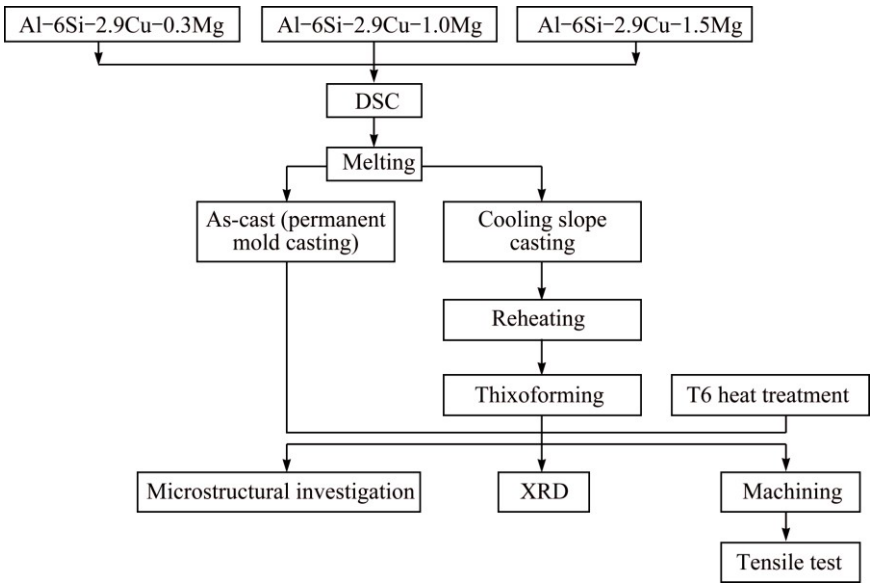

Fig. 1 Process flow chart of experimental procedure

Differential scanning calorimetry (DSC) was employed to estimate the pouring temperature, the solidus and liquidus temperatures and the liquid fraction profile within the semi-solid transition range. The DSC results that were recorded during the melting stage were used to estimate the optimum pouring temperature for the alloys during the CS casting process. The alloys were sectioned into small pieces (approximately 20 mg) for testing with the Netzsch-STA simultaneous thermogravimeter. The samples were heated at 10 °C/min in nitrogen to prevent oxidation. The determination of the fraction liquid with the temperature for the alloys was obtained from the heat flow versus temperature curves shown in Fig. 2.

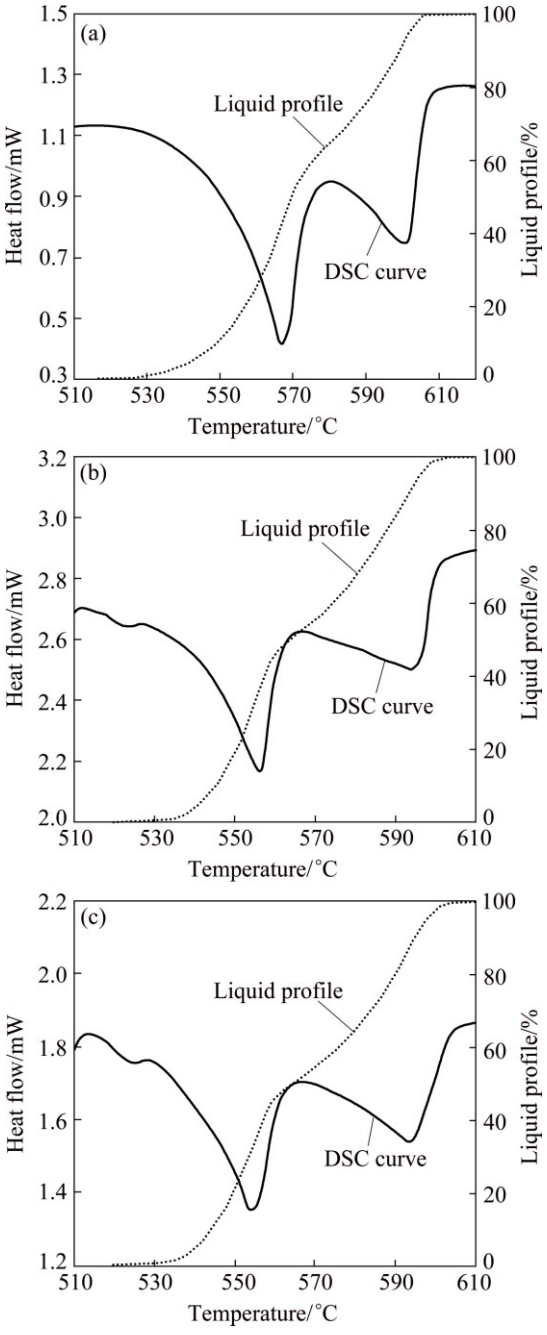

Fig. 2 DSC curves and liquid fraction profiles of alloy A319 (a), alloy TH1 (b) and alloy TH2 (c)

Based on the DSC results, the pouring temperature of 630 °C and CS length of 400 mm were employed in this experiment. The alloys were superheated at 700 °C in a silicon carbide crucible located inside a resistance furnace in an argon atmosphere. The molten alloys were cooled to the pouring temperature before being poured onto the surface of a 90 mm wide inclined plate made of stainless steel (6 mm thick) and were cast into a permanent mould with a diameter of 25 mm and a depth of 110 mm. The surface of the CS was coated with a thin layer of boron nitride to counter act the stickiness of the molten alloy. The tilt angle of 60° of the CS was selected with respect to the horizontal plane and was cooled by water circulation underneath.

Subsequently, the samples produced were heated in a high frequency induction coil to the semi-solid temperature range. The temperature was monitored with a K-type thermocouple inserted in a 5 mm diameter hole drilled at the top of the sample and the frequency of the induction coil was measured to achieve rapid heating (more than 130 °C/min) to avoid grain growth. Some of the samples were isothermally held at their respective semi-solid temperatures obtained from DSC before they were quenched in water. The microstructure of these samples was then analysed in order to determine the optimum reheating temperature and soaking time for the thixoforming process. The thixoforming process was performed using a hydraulic cylinder press that provided a load of 20 kN. The maximum speed for the ram was 85 mm/s and the die (Fig. 3) was preheated to 350 °C. Graphite spray was used as a lubricant to reduce the stickiness between the materials and the die. Some of the thixoformed parts were heat treated to T6 temperature in a salt bath. The solution heat treatment was carried out for 8 h at 505 °C. The solution heat-treated samples were quenched in warm water at 60 °C, and then aged at 158 °C for 4 h.

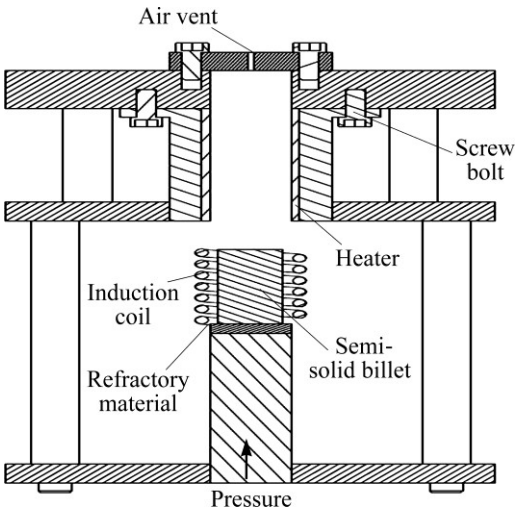

Fig. 3 Schematic diagram of die for thixoforming process

For metallographic preparation, the samples were cut, mounted, ground, polished and then etched with a Keller's reagent for 20 min. Optical micrographs were captured using an Olympus optical microscope (OM), while image analysis, i.e., the calculations of the shape factor (SF) and globule size (GS) of the α(Al) phase, were carried out using Image-J software. The SF is defined as $4\pi A/P^2$, where P is the perimeter and A is the area of the particle (the SF of a circle is equal to one) [22]. The GS of the primary particles is defined as $[\sum 2(A_i/\pi)^{1/2}]/N$, where A_i is the area of each particle and N is the total number of particles in each image [23]. The phases in the alloys were identified using a Carl Zeiss EvoMa 10 scanning electron microscope (SEM) equipped with energy dispersive X-ray (EDX) and X-ray diffraction (XRD).

Cylindrical tensile specimens with typical gauge dimensions of 20 mm in length were machined from the thixoformed and thixoformed T6 samples according to the ASTM-E8M standard. The tensile tests were performed at room temperature using a 100 kN Zwick Roell universal testing machine (UTM). The yield stress was based on a 0.2% plastic strain offset. The fracture surfaces of the tensile samples were investigated using a Carl Zeiss SEM with 100× and 2000× magnifications. By these means, the morphologies of the fractured surface of the thixoformed and thixoformed T6 samples were determined.

3 Results and discussion

3.1 Microstructure investigation

Figure 4 illustrates the as-cast microstructures obtained for all alloys produced in this work. The microstructures of the alloys consisted of α(Al) distributed homogenously in an eutectic matrix. It can be observed that as the Mg content increased (alloys TH1 and TH2), the size of α(Al) was decreased and became less dendritic. It is very clear that Mg can modify the primary α(Al) phase. Figure 5 shows the microstructures of the alloys after they were cast over a CS plate. The changes in the α(Al) phase upon the CS casting are very evident; the dendritic morphology has been replaced by α(Al) globules and rosettes. The shear-driven melt flow along the slope plate is responsible for the change in the shape and morphology of the primary phase [14]. Nucleation started when the molten alloy flowed in the melt contact zone on the slope plate. This was due to the high heat transfer created after pouring the molten alloy onto the slope plate. During the movement of the melt, the exerted shear stress, which is due to gravity, led to the detachment of the newly formed α(Al) phase from the slope surface. Following this, the crystals thus nucleated were detached from the cooling plate and trapped in the flowing melt and then flowed directly into the mould before they evolved into ripened dendrites [24]. The solidified CS microstructure of the billets showed a fine and globular solid α(Al) phase distributed homogenously in the sample. It was evidently shown in Fig. 5 that the CS plate acted as a source of nucleation during the solidification of the Al alloys and was able to produce a suitable Al feedstock for thixoforming.

Fig. 4 Microstructures of as-cast alloys: (a) Alloy A319 (0.3% Mg); (b) Alloy TH1(1.0% Mg); (c) Alloy TH2 (1.5%Mg)

3.2 Isothermal treatment

The semi-solid temperatures used for the thixoforming process were determined from the liquid fraction versus temperature curve, as shown in Fig. 2. Billets with a diameter of 25 mm and a height of 30 mm from alloys A319, TH1 and TH2 produced by CS casting were heated to a semi-solid temperature of 571, 568 and 564 °C, respectively, which corresponded to 50% liquid content. This was done for 5 min in the induction furnace and then rapidly quenched in water in order to get an indication of the evolution of the semi-solid

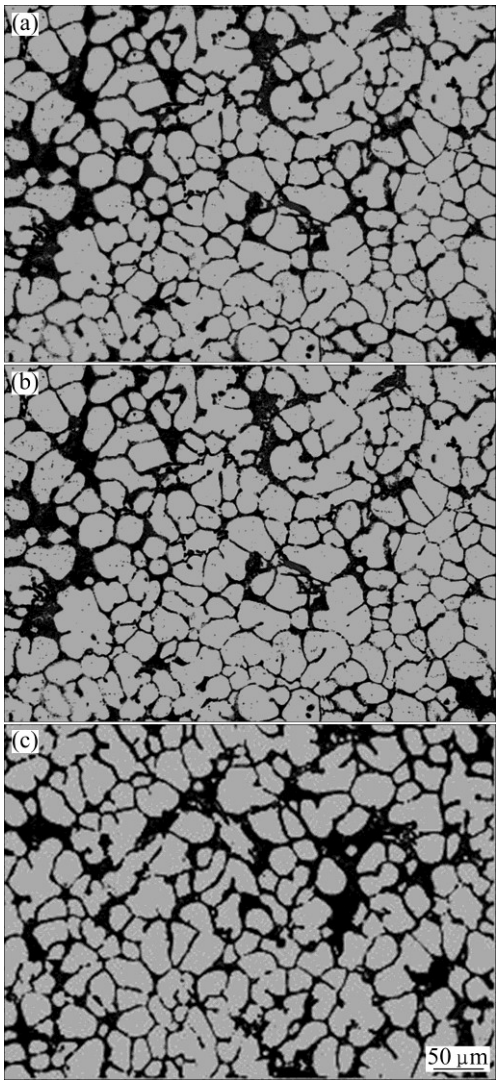

Fig. 5 Microstructures of cooling slope cast alloys: (a) Alloy A319; (b) Alloy TH1; (c) Alloy TH2

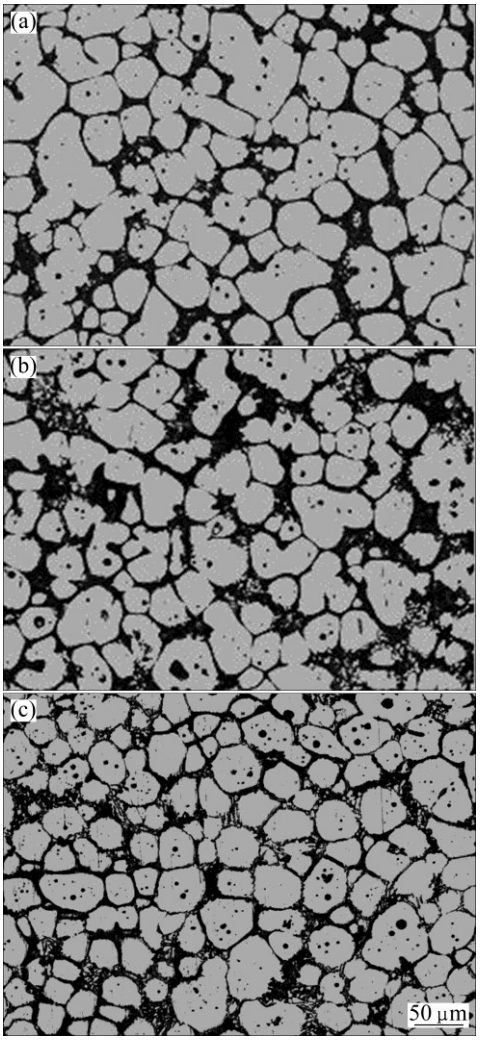

Fig. 6 Microstructures of alloys after being isothermally held at 571 °C for 5 min: (a) Alloy A319; (b) Alloy TH1; (c) Alloy TH2

microstructure at the holding temperature. It was clearly shown at Fig. 6 that the CS billet turned into uniformly distributed globular particles after reheating and isothermal holding at the semi-solid temperature. It was also noticed that the eutectic constituent was melted while all the primary phase remained solid, as represented by the grey colour in Fig. 6. The 5 min of isothermal holding is enough to transform the fine rosette structure from CS casting into a globular microstructure. During the isothermal holding experiment, it was clearly shown that rosette morphology developed a more spheroidal morphology with the development of coalescent necks in the sample.

3.3 Microstructure of thixoformed samples

Figure 7 shows the thixoformed samples of the A319, TH1 and TH2 aluminium alloys at 50% liquid content. As can be seen from Fig. 7, the structure of the samples predominantly consisted of α(Al) globules and Si particles sitting in between these globules. The uniform distribution of the microstructure in these thixoformed samples resulted from segregation of the liquid phase during forming [25]. At a reheating temperature of 50% liquid content, the α(Al) particle remained solid while the eutectic Si was melted during holding. The eutectic Si that melted during reheating was re-arranged during the 5 min holding time and some of the Si and Al were deposited on the primary Si particles and α(Al) [24]. This caused the coarsening process in the α(Al) particles during holding in the semi-solid state. The difference in the globule size of the thixoformed samples is believed to be due to the appropriate heating rates used in thixoforming, which increased the size of the α(Al) phase and also helped with the rounding of the α(Al) grains throughout the samples. It can be realized that the eutectic Si is more effectively modified and refined in alloy TH2 (1.5% Mg) than that in alloy A319 (0.3% Mg) as shown in Figs. 7(a, b) and (e, f), respectively.

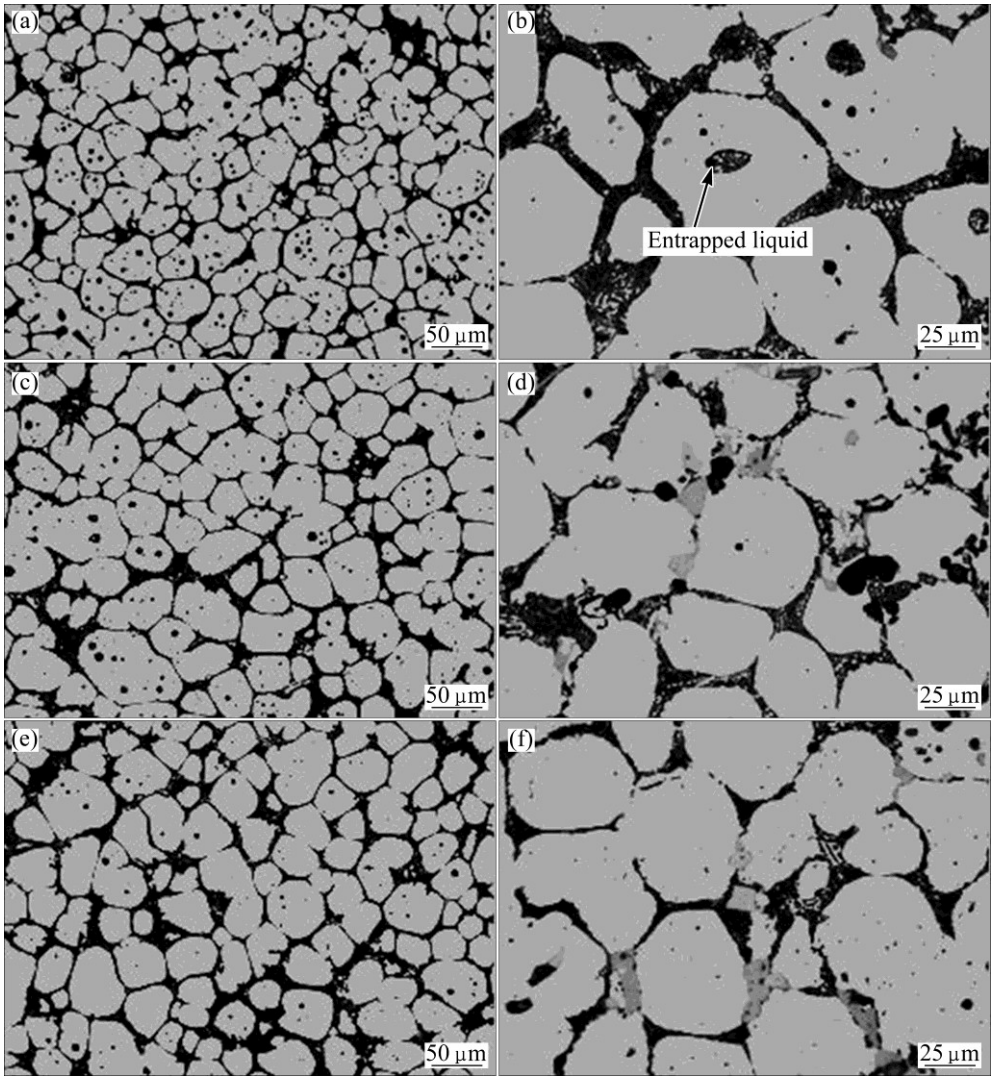

Fig. 7 Microstructures of thixoformed alloys: (a, b) Alloy A319; (c, d) Alloy TH1; (e, f) Alloy TH2

The eutectic of the alloys that contained Si, Al_2Cu and other particles embedded in Al and the shape of these constituents were irregular as in a typical eutectic structure. This is also seen at the higher magnification micrograph in Fig. 7, where some of the liquids were entrapped inside the α(Al) globules. Furthermore, it can be seen that the alloys with low Mg content showed more entrapped liquid during heating, whereas the alloys with higher Mg content showed less entrapped liquid and their structure was more globular. Entrapped liquid is undesirable for thixoforming because it can generate liquid inside the α(Al) globules when the material is reheated to the semi-solid state, thus disrupting the lubrication process which is very important for generating semi-solid behavior during thixoforming [26]. Figure 8 shows the GS and SF of the thixoformed alloys. It can be seen clearly that alloy TH2, which contains 1.5% Mg, recorded the highest SF of about 0.9 while the GS was about 53.5 μm.

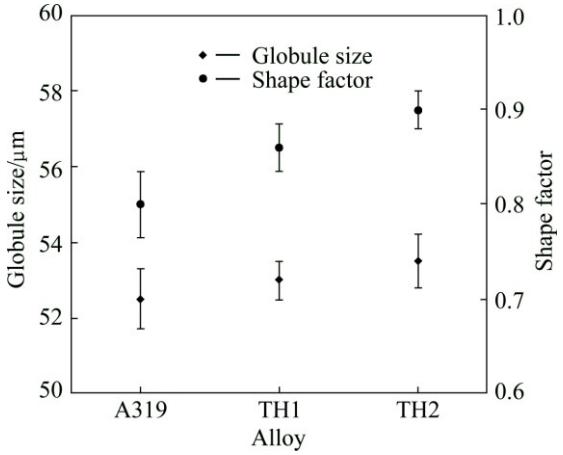

Fig. 8 Globule size and shape factor of thixoformed alloys

The thixoformed alloys samples were subjected to T6 heat treatment in order to enhance their mechanical properties. The T6 treatment had an impact on the microstructure as it modified the Si particles that were embedded around the α(Al) globules, as shown in Fig. 9.

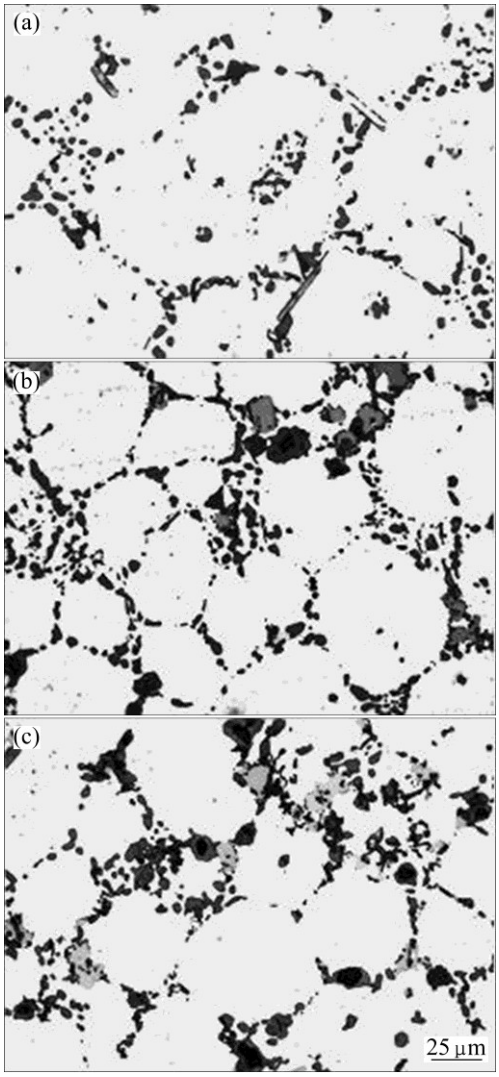

Fig. 9 Microstructures of thixoformed alloys after T6 heat treatment: (a) Alloy A319; (b) Alloy TH1; (c) Alloy TH2

During solution treatment at 505 °C, some physical changes occurred, i.e., coarsening and spheroidization of the Si particles, formation of small participates inside the solid phase and a dissolving of the Cu-rich phase inside the eutectic region. Coarsening is attributed to the residual particles that are produced during the dissolution process. The dissolution process is very important because it can maximize the content and distribution of Si, Cu and Mg in a solid solution as it can help to obtain maximum yield strength [27]. The presence of Si particles of rounded shape showed that there was an evolution of the eutectic Si morphology caused by thixoforming process [28]. Moreover, the fine Si particles generated in the eutectic phase are related to the effect of iron phase during thixoforming process [29]. After solution treatment, the samples were quenched in warm water and then they were aged at 158 °C for 4 h. As can be seen from Fig. 9, the aged alloy samples exhibit precipitation of Al_2Cu and Mg_2Si phase in their metastable form. Moreover, it was clearly seen in Figs. 9(b) and (c) that the alloys TH1 and TH2 have higher precipitation in the intermetallic phase when compared to the alloy A319. This is due to the higher amount of Mg in TH1 and TH2. There was also a homogenous distribution of the precipitated particles throughout the matrix in the T6 samples.

Figures 10 and 11 represent the SEM-EDX elemental mapping of alloy TH1 in the thixoformed and thixoformed T6 conditions, respectively. In the thixoformed condition, Si Cu, Mg, Mn and Fe were intensified in certain regions within the Al matrix while in the thixoformed T6 condition, as shown in Fig. 11, Si was spheroidized in certain regions within the globules and Cu, Mg, Fe and Mn were distributed homogenously in the sample. Microstructural characterization of the thixoformed samples was carried out using SEM back scatter analysis (BSE).

Figures 12 and 13 display the SEM images and EDX patterns for alloy TH2 in thixoformed and thixoformed T6 condition, respectively. The EDX analysis result indicates the existence of a small amount of Si, Cu, Mg and Fe elements in the Al matrix. These elements accumulated heavily in the eutectic phase at the grain boundaries. Figure 14 shows SEM images for the alloys A319, TH1 and TH2 in thixoformed and thixoformed T6 conditions. Figure 14(a) shows that the A319 alloy contains Al_2Cu, $Al_5Cu_2Mg_8Si_5$ and β-Al_5FeSi phases that are present in the eutectic region while in alloys TH1 and TH2, as shown in Figs. 14(b) and (c), respectively, new phases of Mg_2Si and $Al_9FeMg_3Si_5$ were detected. These intermetallic compounds were confirmed by XRD analysis as shown in Fig. 15. In alloy A319, all of the Mg atoms reacted with Cu atoms to produce $Al_5Cu_2Mg_8Si_5$ during alloy solidification. In the case of alloys TH1 and TH2, some of the Mg atoms reacted with Si atoms to produce a Mg_2Si phase and the remaining Mg atoms reacted with Cu and Fe to produce an $Al_5Cu_2Mg_8Si_5$ and $Al_9FeMg_3Si_5$ intermetallic compound, respectivelys. According to MOHAMED et al [30], the $Al_9FeMg_3Si_5$ compound has a compact morphology which is detrimental to an alloy's tensile properties, expecially elongation to fracture.

The microstrutcure of a sample obtained after T6 heat treatment is shown in Figs. 14(d)−(f). In the thixoformed T6 sample, the particle distribution has improved relative to those of the as-thixoformed samples and the Si particles have completely transformed into the spheoridal form. The T6 heat treatment had an impact on the microstructure as it helped to spheroidize the Si particles during solution treatment at 505°C and developed intra-granular contrast during ageing at 158 °C [24]. The structure of the thixoformed T6 alloys showed the dispersion of fine Si particles and an Al_2Cu

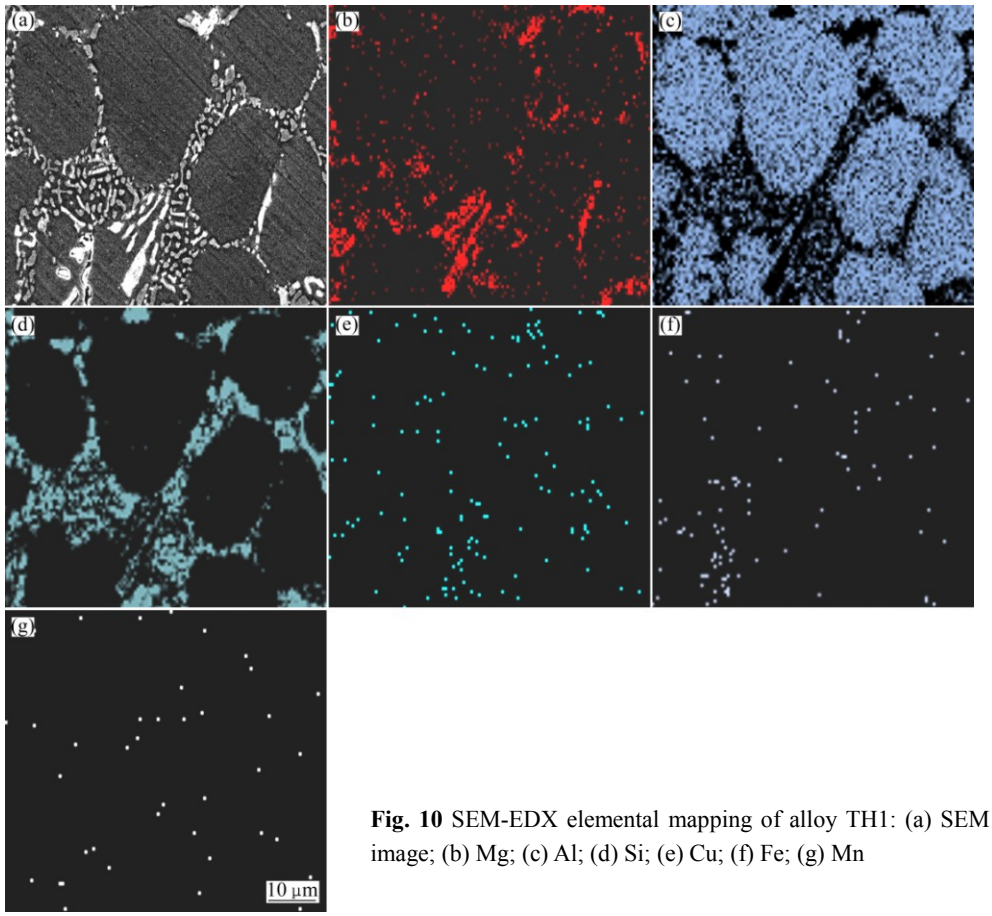

Fig. 10 SEM-EDX elemental mapping of alloy TH1: (a) SEM image; (b) Mg; (c) Al; (d) Si; (e) Cu; (f) Fe; (g) Mn

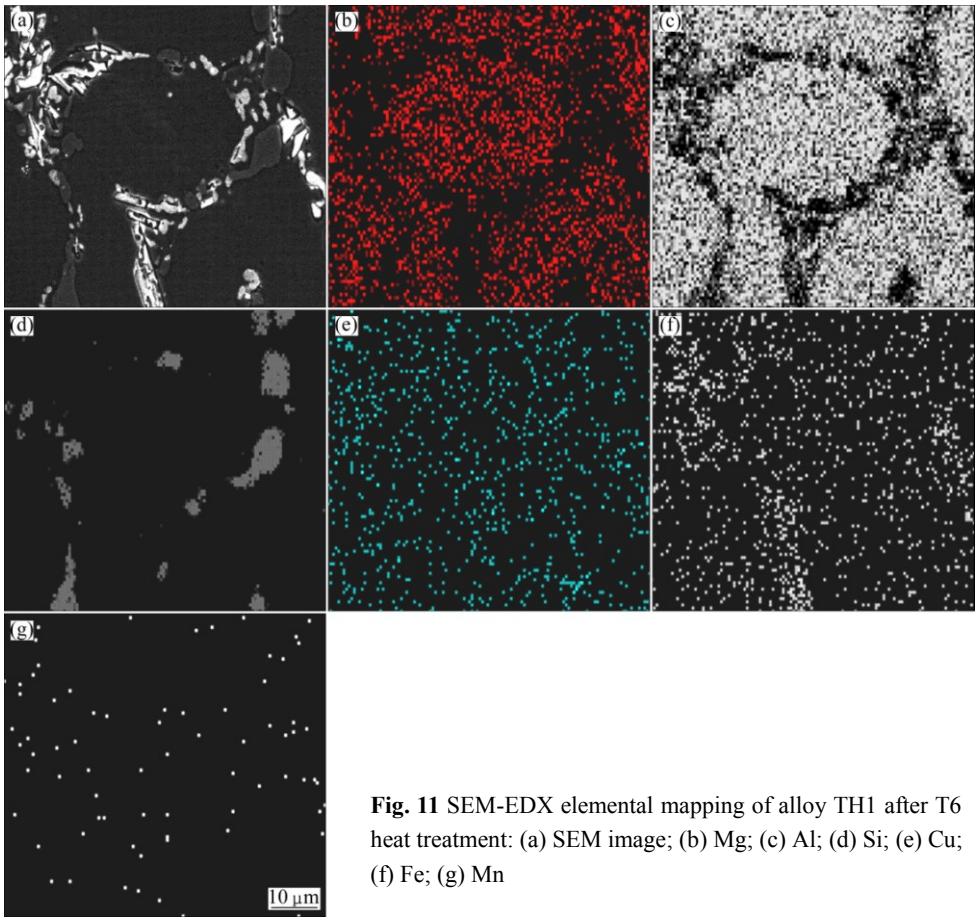

Fig. 11 SEM-EDX elemental mapping of alloy TH1 after T6 heat treatment: (a) SEM image; (b) Mg; (c) Al; (d) Si; (e) Cu; (f) Fe; (g) Mn

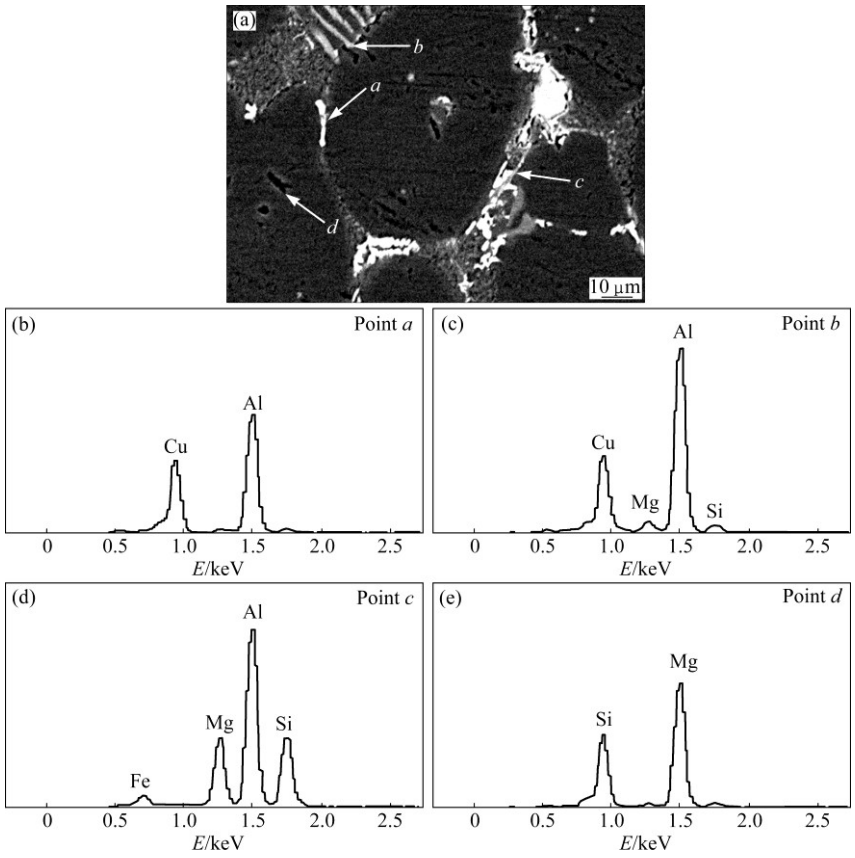

Fig. 12 SEM-EDX analysis of thixoformed alloy TH2 (Note: point *a*, Al_2Cu; point *b*, $Al_5Cu_2Mg_3Si_5$; point *c*, $Al_9FeMg_3Si_5$; point *d*, Mg_2Si)

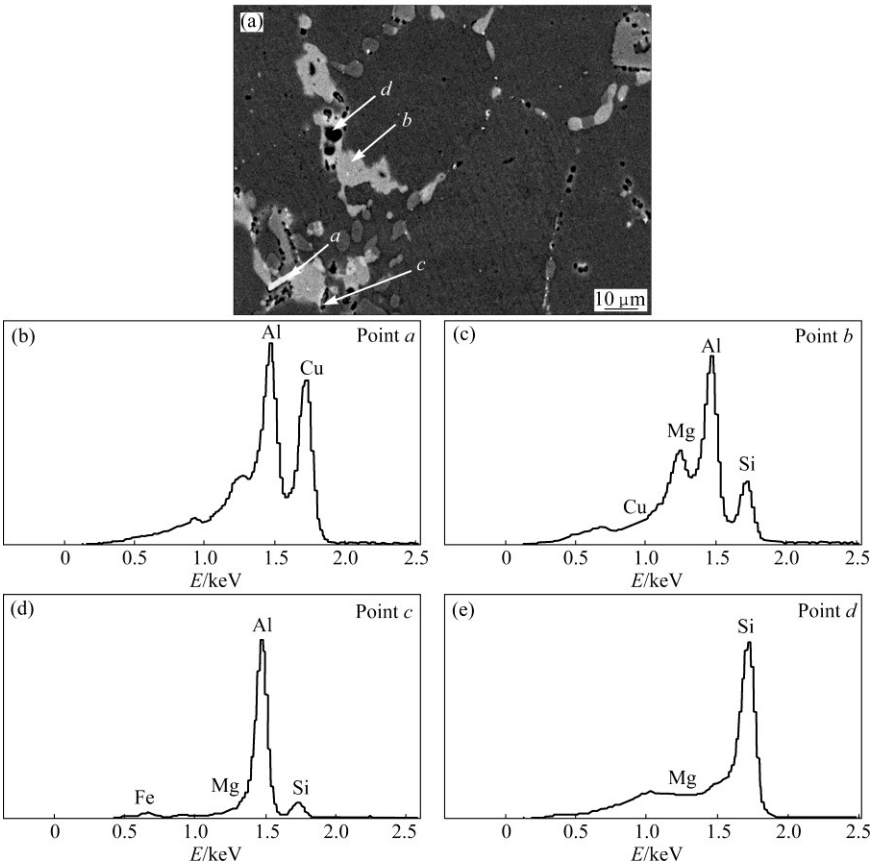

Fig. 13 SEM-EDX analysis of thixoformed alloy TH2 after T6 treatment (Note: point *a*, Al_2Cu; point *b*, $Al_5Cu_2Mg_3Si_5$, point *c*, $Al_9FeMg_3Si_5$, point *d*, Mg_2Si)

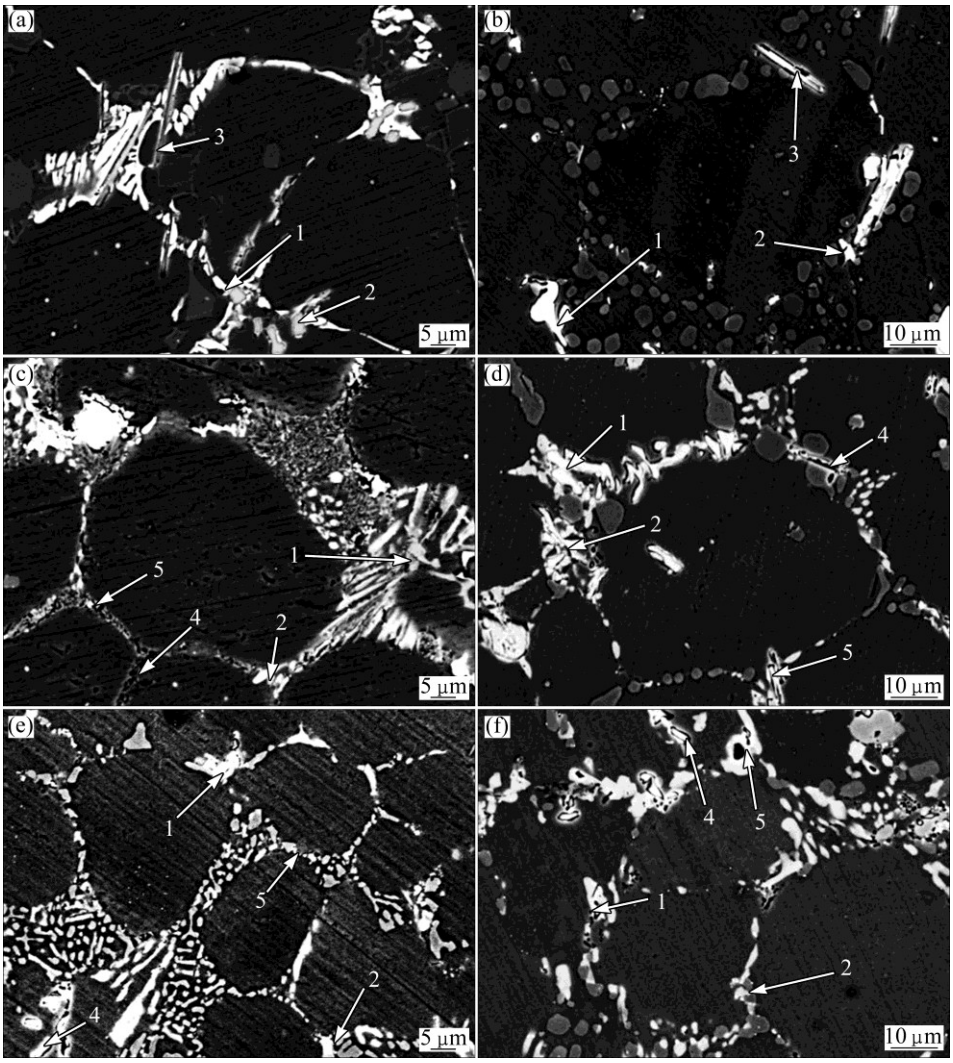

Fig. 14 SEM backscatter electron images of thixoformed alloys: (a) Alloy A319; (b) Alloy TH1; (c) Alloy TH2; (d) Alloy A319-T6; (e) Alloy TH1-T6; (f) Alloy TH2-T6 (Note: 1=Al_2Cu, 2= $Al_5Cu_2Mg_3Si_5$, 3=β-Al_5FeSi, 4= $Al_9FeMg_3Si_5$, 5= Mg_2Si)

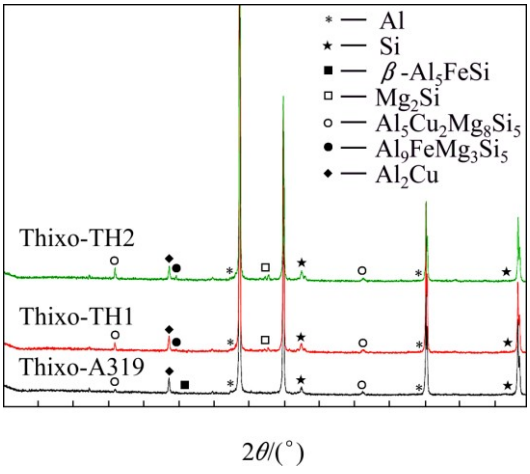

Fig. 15 XRD patterns of thixoformed alloys

intermetallic phase embedded around the α(Al) globules and the particle distribution including intermetallic compounds was more homogenous after T6 heat treatment. Small amounts of Mg_2Si were precipitated alongside the Si particles dispersed homogenously throughout the samples, which may have improved the mechanical properties of the alloy [18].

3.4 Tensile properties

Figures 16 and 17 show the tensile test results and elongation to fracture, respectively, for the alloys A319 in as-cast, as-thixoformed and thixoformed T6. As shown in Fig. 16, for the thixoformed sample A319, the ultimate tensile strength and yield strength were 241 MPa and 176 MPa, respectively, while the elongation to fracture (Fig. 17) was 3.2%. For the thixoformed alloy TH1, which contained 1.0% Mg, the ultimate tensile strength, yield strength and elongation to fracture were 260 MPa, 216 MPa, and 1.5%, respectively, while for alloy TH2, that contained 1.5% Mg, the ultimate tensile strength, yield strength and elongation to fracture were 281 MPa, 237 MPa and 0.8%, respectively.

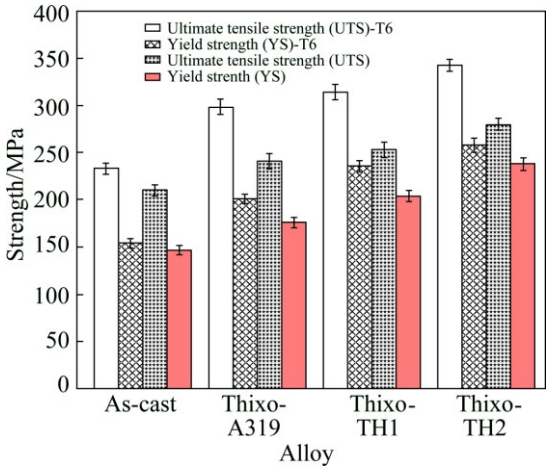

Fig. 16 Comparison of ultimate tensile strength and yield strength of thixoformed and thixoformed T6 alloys

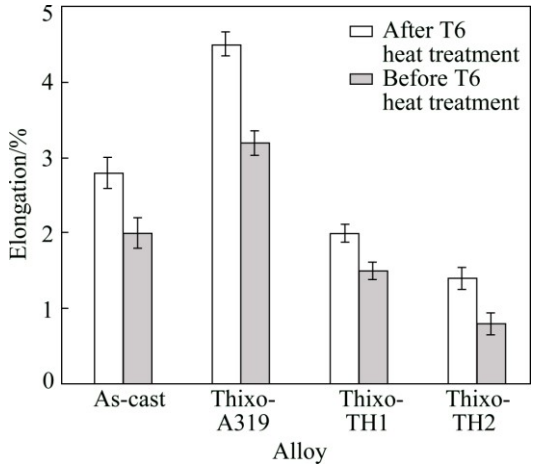

Fig. 17 Comparison of tensile elongation of as-thixoformed and thixoformed T6 alloys

The same patterns were also observed after T6 heat treatment, as shown in Figs. 16 and 17. For the thixoformed A319 alloy, the ultimate tensile strength, yield strength and elongation to fracture were 298 MPa, 201 MPa and 4.5%, respectively. In the case of alloy TH1, the ultimate tensile strength, yield strength and elongation to fracture were increased to 311 MPa, 237 MPa and 2.1%, respectively, while for alloy TH2, the ultimate tensile strength, yield strength and elongation to fracture were increased to 325 MPa, 251 MPa and 1.4%, respectively. As expected, increasing the Mg amount resulted in the reduction of elongation to fracture in the thixoformed alloys. The reduction of elongation to fracture is attributed to the formation of more Mg_2Si as well as the changes in the Fe-rich intermetallic compounds ($Al_9FeMg_3Si_5$) that form in the alloys with increasing Mg content. Furthermore, T6 heat treatment, which gave a good response in the formation of more Mg_2Si and Al_2Cu precipitates in the Al matrix, also contributes to the increase of strength. The precipitation sequence of Mg_2Si that emerges in the structure after the addition of Mg to Al−Si alloys is as follows [31]:

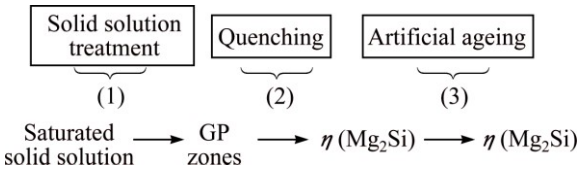

Saturated solid solution was obtained by heating the alloy to its solvus temperature and then quenching it to form GP zones. The instable and consistent phase η(Mg_2Si) and stable and inconsistent phase η (Mg_2Si) was obtained after the ageing treatment. The η (Mg_2Si) phase that was formed at the end of the sequence, made the dislocation movement more difficult, and as a result, the tensile strengths of the alloys were increased. On the other hand, this situation led to the reduction in the ductility of the alloys. It is evident from Fig. 17 that the elongation to fracture was reduced as the Mg content was increased.

3.5 Fracture surface analysis

Fracture surface analysis was performed on the tensile fractured samples of the thixoformed and thixoformed T6 alloys in order to understand the fracture mechanism that occurred during tensile testing. As can be seen in Fig. 18(a), the thixoformed A319 alloy has a ductile fracture as evidenced from the cellular morphology type fracture that is dominated by a dimple structure, which is believed to have good ductility. In contrast, the fractographs of alloys TH1 and TH2 in Figs. 18(b) and (c) show a combination of ductile and cleavage ruptures, respectively. This type of fracture reduces the ductility of the alloys as evidenced by the tensile results presented in Fig. 17.

As discussed in the previous section, T6 heat treatment helped to increase the precipitation of fine Al_2Cu and Mg_2Si, which help to improve the mechanical properties of the alloys. Solution treatment at 505 °C for 8 h resulted in partial spheroidization of the Si particles and provided a large surface area of ductile Al matrix. Moreover, dissolution of a large proportion of Cu and Mg occurred during this solution treatment. After the solution treatment, the samples were aged at 158 °C for 4 h and this introduced noticeable changes in the general rupture features. As shown in Fig. 18(d), the T6 treated A319 alloys were dominated by dimple structure, and the crack occurred by void initiation at the Si particle, which helped to improve the ductility of the T6 thixoformed alloy. In the case of alloys TH1 and TH2, as shown in

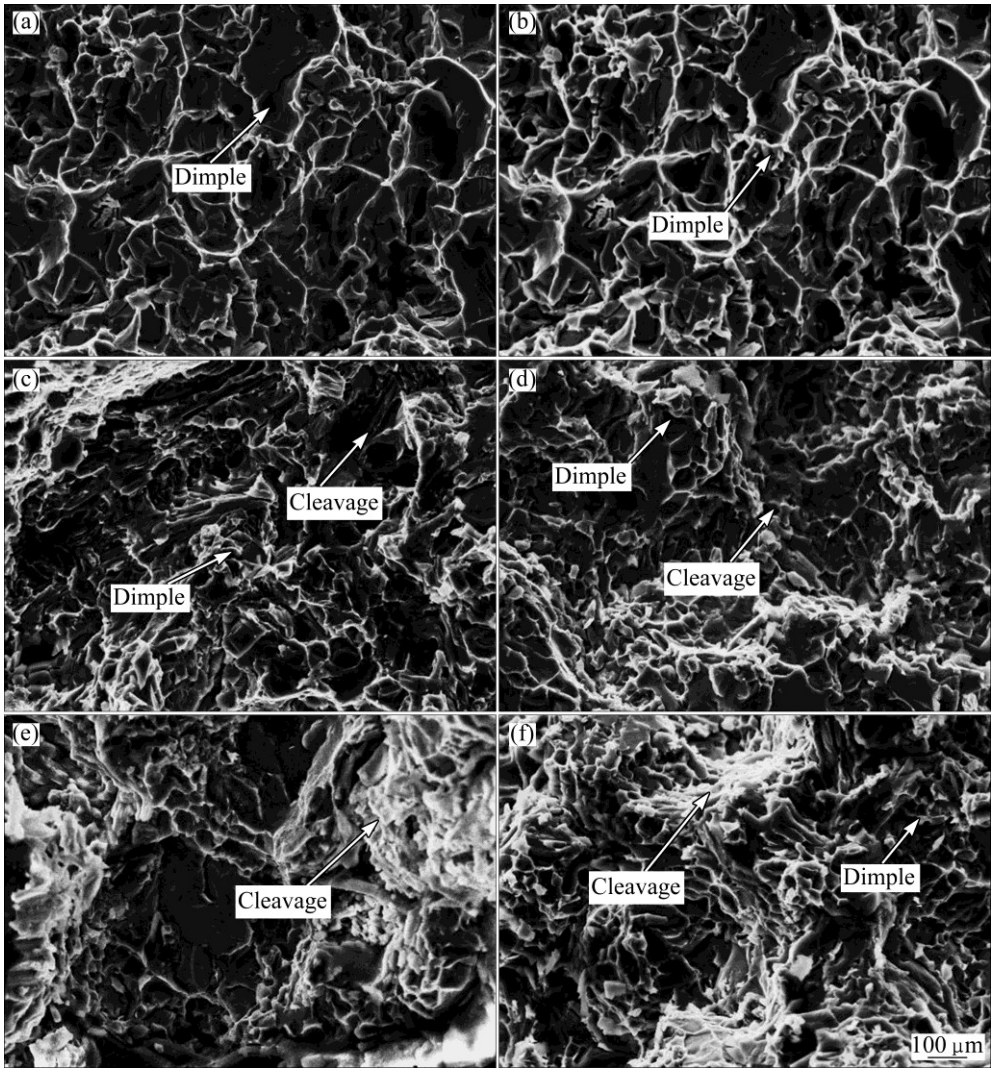

Fig. 18 SEM images of fracture surface of thixoformed alloys: (a) Alloy A319; (b) Alloy TH1; (c) Alloy TH2; (d) Alloy A319-T6; (e) Alloy TH1-T6; (f) Alloy TH2-T6

Figs. 18(e) and (f), respectively, the fracture samples show a cleavage rupture resulted from brittle fracture behavior. Crack propagation between α(Al) grains, which is believed to originate in the Si, Fe and Mg containing phase, reducing the elongation to fracture of thixoformed alloys TH1 and TH2.

4 Conclusions

1) It was observed that the A319 alloys containing various amounts of Mg are suitable for the thixoforming process. Increasing the Mg content in A319 alloy up to 1.5% enhanced the alloy response to T6 heat treatment. Moreover, addition of 1.0% and 1.5% Mg resulted in the formation of Mg_2Si and Fe-rich intermetallic compound $Al_9FeMg_3Si_5$ in the alloys.

2) It was determined that the addition of Mg to A319 alloy resulted in slightly refining the size of silicon eutectic in the alloys.

3) The alloy with the highest Mg content had the highest tensile strength but this amount of Mg reduced the elongation to fracture of the alloy. The tensile properties of the T6 heat treated A319 alloy samples showed a significant improvement when Mg was added. The ultimate and tensile strengths recorded were as high as 325 MPa and 251 MPa, respectively, in alloys that contained 1.5% Mg. However, the elongation to fracture was reduced to 1.4%.

4) The A319 alloys showed a ductile fracture behaviour while the alloys with 1.0% Mg and 1.5% Mg showed a mixed mode fracture behaviour, where dimple and cleavage ruptures were seen on the fracture surface of the sample. The thixoformed alloys subjected to T6 heat treatment showed a mixed mode fracture behaviour, where a dimpled structure was dominant in the samples. This indicates that the T6 thixoformed samples have improved material ductility relative to the thixoformed samples.

Acknowledgements

The authors would like to thank the Universiti Teknikal Malaysia Melaka (UTeM) and the Ministry of Education, Malaysia for being financial sponsors of this study. Much appreciation also goes to Universiti Kebangsaan Malaysia (UKM) for the financial support under research grants GUP-2012-040 and AP-2012-014.

References

[1] TAVITAS-MEDRANO F J, GRUZLESKI J E, SAMUEL F H, VALTIERRA S, DOTY H W. Effect of Mg and Sr-modification on the mechanical properties of 319-type aluminum cast alloys subjected to artificial aging [J]. Materials Science and Engineering A, 2008, 480: 356−364.

[2] ALHAWARI K S, OMAR M Z, GHAZALI M J, SALLEH M S, MOHAMMED M N. Evaluation of the microstructure and dry sliding wear behaviour of thixoformed A319 aluminium alloy [J]. Materials & Design, 2015, 76: 169−180.

[3] RINCÓN E, LÓPEZ H F, CISNEROS M M, MANCHA H, CISNEROS M A. Effect of temperature on the tensile properties of an as-cast aluminum alloy A319 [J]. Materials Science and Engineering A, 2007, 452−453: 682−687.

[4] SALLEH M S, OMAR M Z, SYARIF J, MOHAMMED M N, ALHAWARI K S. Thermodynamic simulation on thixoformability of aluminium alloys for semi-solid metal processing [J]. International Journal of Mathematics and Computers in Simulation, 2013, 7: 286−293.

[5] NAFISI S, GHOMASHCHI R. Grain refining of conventional and semi-solid A356 Al−Si alloy [J]. Journal of Materials Processing Technology, 2006, 174: 371−383.

[6] OMAR M Z, PALMIERE E J, HOWE A A, ATKINSON H V, KAPRANOS P. Thixoforming of a high performance HP9/4/30 steel [J]. Materials Science and Engineering A, 2005, 395: 53−61.

[7] TAHAMTAN S, FADAVI BOOSTANI A. Microstructural characteristics of thixoforged A356 alloy in mushy state [J]. Transactions of Nonferrous Metals Society of China, 2010, 20(S3): s781−s787.

[8] SALLEH M S, OMAR M Z, SYARIF J, ALHAWARI K S, MOHAMMED M N. Microstructure and mechanical properties of thixoformed A319 aluminium alloy [J]. Materials & Design, 2014, 64: 142−152.

[9] SALLEH M S, OMAR M Z, SYARIF J, MOHAMMED M N. An overview of semisolid processing of aluminium alloys [J]. ISRN Materials Science, 2013, 2013: 1−9.

[10] OMAR M Z, ATKINSON H V, KAPRANOS P. Thixotropy in semisolid steel slurries under rapid compression [J]. Metallurgical and Materials Transactions A: Physical Metallurgy and Materials Science, 2011, 42: 2807−2819.

[11] ZOQUI E J, NALDI M A. Evaluation of the thixoformability of the A332 Alloy (Al−9.5wt%Si−2.5 wt%Cu) [J]. Journal of Materials Science, 2011, 46: 7558−7566.

[12] PARK C, KIM S, KWON Y, LEE Y, LEE J. Mechanical and corrosion properties of rheocast and low-pressure cast A356-T6 alloy [J]. Materials Science and Engineering A, 2005, 391: 86−94.

[13] TAHAMTAN S, FADAVI BOOSTANI A. Quantitative analysis of pitting corrosion behavior of thixoformed A356 alloy in chloride medium using electrochemical techniques [J]. Materials & Design, 2009, 30: 2483−2489.

[14] BIROL Y. A357 thixoforming feedstock produced by cooling slope casting [J]. Journal of Materials Processing Technology, 2007, 186: 94−101.

[15] MOHAMMED M N, OMAR M Z, SALLEH M S, ALHAWARI K S, KAPRANOS P. Semisolid metal processing techniques for nondendritic feedstock production [J]. The Scientific World Journal, 2013, 2013: 1−16.

[16] BIROL Y, AKDI S. Cooling slope casting to produce EN AW 6082 forging stock for manufacture of suspension components [J]. Transactions of Nonferrous Metals Society of China, 2014, 24: 1674−1682.

[17] ATKINSON H V. Semisolid processing of metallic materials [J]. Materials Science and Technology, 2010, 26: 1401−1413.

[18] SALLEH M S, OMAR M Z, SYARIF J. The effects of Mg addition on the microstructure and mechanical properties of thixoformed Al−5%Si−Cu alloys [J]. Journal of Alloys and Compounds, 2015, 621: 121−130.

[19] ALKAHTANI S. Mechanical performance of heat treated 319 alloys as a function of alloying and aging parameters [J]. Materials & Design, 2012, 41: 358−369.

[20] RINCON E, LOPEZ H F, CISNEROS M M, MANCHA H. Temperature effects on the tensile properties of cast and heat treated aluminum alloy A319 [J]. Materials Science and Engineering A, 2009, 519: 128−140.

[21] WU C T, LEE S L, HSIEH M H, LIN J C. Effects of Cu content on microstructure and mechanical properties of Al−14.5Si−0.5Mg alloy [J]. Materials Characterization, 2010, 61: 1074−1079.

[22] ARIF M A M, OMAR M Z, MUHAMAD N, SYARIF J, KAPRANOS P. Microstructural evolution of solid-solution-treated Zn−22Al in the semisolid state [J]. Journal of Materials Science & Technology, 2013, 29: 765−774.

[23] CZERWINSKI F. On the generation of thixotropic structures during melting of Mg−9%Al−1%Zn alloy [J]. Acta Materialia, 2002, 50: 3265−3281.

[24] BIROL Y. Semi-solid processing of the primary aluminium die casting alloy A365 [J]. Journal of Alloys and Compounds, 2009, 473: 133−138.

[25] BIROL Y. Evolution of globular microstructures during processing of aluminium slurries [J]. Transactions of Nonferrous Metals Society of China, 2013, 23: 1−6.

[26] PAES M, ZOQUI E J. Semi-solid behavior of new Al−Si−Mg alloys for thixoforming [J]. Materials Science and Engineering A, 2005, 406: 63−73.

[27] OUELLET P, SAMUEL F H. Effect of Mg on the ageing behaviour of Al−Si−Cu 319 type aluminium casting alloys [J]. Journal of Materials Science, 1999, 34: 4671−4697.

[28] FADAVI BOOSTANI A, TAHAMTAN S. Microstructure and mechanical properties of A356 thixoformed alloys in comparison with gravity cast ones using new criterion [J]. Transactions of Nonferrous Metals Society of China, 2010, 20: 1608−1614.

[29] FADAVI BOOSTANI A, TAHAMTAN S. Effect of a novel thixoforming process on the microstructure and fracture behavior of A356 aluminum alloy [J]. Materials & Design, 2010, 31: 3769−7376.

[30] MOHAMED A M A, SAMUEL F H, AL KAHTANI S. Influence of Mg and solution heat treatment on the occurrence of incipient melting in Al−Si−Cu−Mg cast alloys [J]. Materials Science and Engineering A, 2012, 543: 22−34.

[31] LI R X, LI R D, ZHAO Y H, HE L Z, LI C X, GUAN H R. Age-hardening behavior of cast Al–Si base alloy [J]. Materials Letters, 2004, 58: 2096−2101.

镁含量对触变成形 A319 合金显微组织演变和力学性能的影响

M. S. SALLEH[1], M. Z. OMAR[2], K. S. ALHAWARI[2], M. N. MOHAMMED[3], M. A. MAD ALI[1], E. MOHAMAD[1]

1. Department of Manufacturing Process, Faculty of Manufacturing Engineering, Universiti Teknikal Malaysia Melaka, Hang Tuah Jaya, 76100 Durian Tunggal Melaka, Malaysia;
2. Department of Mechanical and Materials Engineering, Faculty of Engineering and Built Environment, Universiti Kebangsaan Malaysia, 43600, Selangor, Malaysia;
3. Department of Engineering and Technology, Faculty of Information Sciences and Engineering, Management and Science University, 40100 Shah Alam, Selangor, Malaysia

摘　要：研究不同镁含量对触变成形 A319 合金显微组织和拉伸性能的影响。合金在含 50%液相时进行触变成形，并对部分合金进行 T6 热处理。采用光学显微镜、扫描电子显微镜、能量散射谱、X 射线衍射和拉伸试验对合金进行表征。结果表明，镁可以细化合金中共晶硅。当镁含量为 1.0% 和 1.5%时，合金中形成致密的 $Al_9FeMg_3Si_5$ 相。随着镁含量的增加，触变成形合金的拉伸强度增加。热处理后的触变成形 A319 合金的抗拉强度、屈服强度和伸长率分别为 298 MPa，201 MPa 和 4.5%。而对于添加 1.5%Mg 的触变成形 A319 合金，其热处理后的抗拉强度、屈服强度和伸长率分别为 325 Pa、251 MPa 和 1.4%。触变成形 A319 合金表现为韧窝断裂，而添加 1.5%Mg 的 A319 合金表现为混合断裂，在合金表面可观察到韧窝断裂和解理断裂。

关键词：铝合金；触变成形；T6 热处理；力学性能

(Edited by Yun-bin HE)